

# Asynchronous Message Passing for Addressing Oversquashing in Graph Neural Networks

Kushal Bose and Swagatam Das

## Abstract

Graph Neural Networks (GNNs) suffer from Oversquashing, which occurs when tasks require long-range interactions. The problem arises from the presence of bottlenecks that limit the propagation of messages among distant nodes. Recently, graph rewiring methods modify edge connectivity and are expected to perform well on long-range tasks. Yet, graph rewiring compromises the inductive bias, incurring significant information loss in solving the downstream task. Furthermore, increasing channel capacity may overcome information bottlenecks but enhance the parameter complexity of the model. To alleviate these shortcomings, we propose an efficient model-agnostic framework that asynchronously updates node features, unlike traditional synchronous message passing GNNs. Our framework creates node batches in every layer based on the node centrality values. The features of the nodes belonging to these batches will only get updated. Asynchronous message updates process information sequentially across layers, avoiding simultaneous compression into fixed-capacity channels. We also theoretically establish that our proposed framework maintains higher feature sensitivity bounds compared to standard synchronous approaches. Our framework is applied to six standard graph datasets and two long-range datasets to perform graph classification and achieves impressive performances with a 5% and 4% improvements on REDDIT-BINARY and Peptides-struct, respectively.

## Index Terms

Graph, Convolution, Message passing, Oversquashing, Centrality, Asynchronization, Oversmoothing

## 1 INTRODUCTION

Graph Neural Networks [1], [2], [3] predominantly aggregate localized information, which proves to be insufficient for tasks requiring long-range interactions, like molecular property predictions [4], [5]. The interactions between the multi-hop nodes [6] can be leveraged by enhancing the size of neighborhoods. Yet, the increasing number of neighbors introduces the problem of compressing the growing amount of information in the fixed-dimensional vectors, which creates information bottlenecks. This phenomenon is commonly known as *Oversquashing* [7], [8] that causes significant information loss, particularly affecting signals from distant nodes, crucial for the downstream task [9].

**Limitations of Related Works.** Mitigating oversquashing begins with converting the input graph into a fully connected (FA) graph [7] and applying it to either the final layer or every layer of the base GNN model. Recent approaches have attempted to address oversquashing through graph rewiring methods [10], [11], [12], [13], [14], [15], which add edges as “shortcuts” between long-distance nodes to facilitate multi-hop information flow. Nevertheless, FA or rewiring methods tamper with the original graph topology, potentially compromising the inductive bias and incurring information loss. As an alternative avenue, Graph Transformers (GTs) [16] enable global message passing between all pairs of nodes, but they introduce prohibitive computational complexity, particularly for large graphs. More recently, PANDA [17] proposed expanding the feature dimensions of high-centrality nodes. However, this approach increases model parameters and discards potentially valuable information when selecting top-ranked features.

**Motivation** To eliminate those limitations, we design an efficient asynchronous message passing strategy that selectively updates node features across layers, unlike standard message passing architectures like GCN [18], GAT [19], GCNII [20], etc. To the best of our knowledge, we are the first to introduce a novel asynchronous message passing framework to combat oversquashing. Our framework creates node batches in every layer based on some pre-defined criterion and updates features of the nodes belonging to those batches. In contrast, unselected nodes preserve their features from previous layers. Recently, GwAC [21] processes messages from nodes to their neighboring nodes at different times. Yet, this method overlooks the channel capacity and offers no solution to tackle oversquashing. On the contrary, our asynchronous framework explicitly manages fixed-capacity channels by accessing aggregated messages at some particular layer, preventing information overflow. This layer-dependent access prevents simultaneous compression of vast amounts of information, effectively utilizing the same channel capacity without modifying graph topology or increasing the model parameters.

• Electronics and Communication Sciences Unit, Indian Statistical Institute, Kolkata, India.

E-mail: kushalbose92@gmail.com, swagatam.das@isical.ac.in

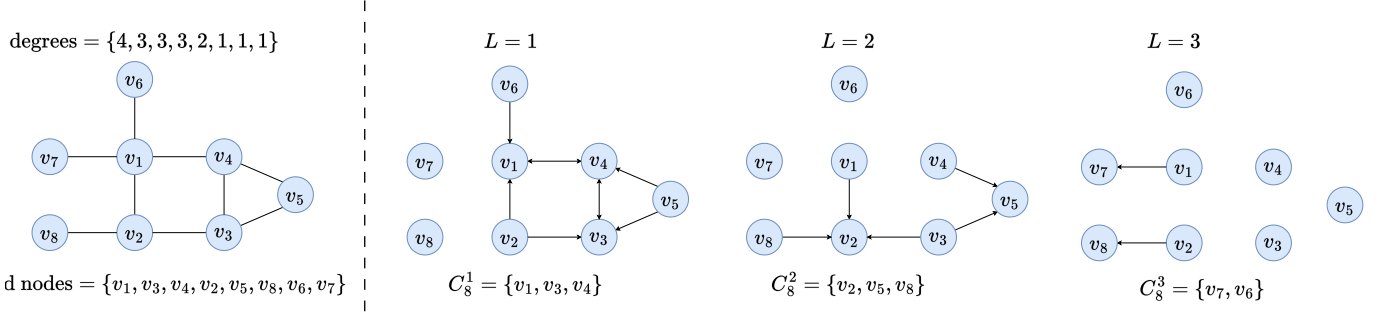


Fig. 1: The workflow of CAMP is presented. The degree centrality values are sorted in descending order. For a 3-layered GNN model, the centrality set is divided into three disjoint subsets. In each layer, the features of the nodes belonging to the pertinent subset are updated. Graph adjacency alters at every layer, and the updated node features are carried forward to the next layer.

In this work, we propose a novel plug-and-play framework **Centrality-aware Asynchronous Message Passing** or **CAMP** that adopts node centrality (degree, betweenness, etc) as our selection criterion to create node batches. CAMP performs ordering (ascending or descending) of the node centrality values and partitions the whole set into multiple disjoint subsets, each corresponding to a distinct message-passing layer. The complete workflow is illustrated in Figure 1. This partitioning ensures that every node gets a chance to exchange messages with its neighbors at some layer. In a network, the high-centrality nodes are regarded as potential bottlenecks in message propagation. By processing these critical nodes earlier, CAMP allows their updated representations to flow to low-centrality nodes in subsequent layers. This approach strategically manages the information flow through these bottleneck nodes. Thus, asynchronous feature updates prevent the simultaneous compression of exponentially growing neighborhood information into fixed-capacity channels, diminishing the effect of oversquashing. We also offer theoretical underpinnings to validate the efficacy of our proposed framework. Unlike PANDA, our framework does not require increasing the dimension of node features, thereby asserting learning in a low-parameter regime. Notably, PANDA performs synchronous message updates, which strictly differ from CAMP.

**Contribution** Our contributions are summarized as:

- **Asynchronous Message Passing** We design a generalized framework for performing asynchronous message passing that departs from the conventional synchronous updates in standard GNNs. The framework selects node batches at each layer based on pre-defined criteria and updates only those features, with CAMP specifically using node centrality measures to guide batch selection. Our approach seamlessly integrates with diverse GNN architectures as a plug-and-play solution.
- **Oversquashing Mitigation** Asynchronous message updates enable the processing of larger volumes of information through fixed-capacity channels at different layers. This prevents the simultaneous compression of exponentially growing information into fixed-sized vectors, effectively addressing the oversquashing without increasing model parameters or modifying graph structure.
- **Theoretical Insights** We provide a theoretical analysis demonstrating that CAMP mitigates oversquashing by enhancing feature sensitivity through its asynchronous updates.

## 2 RELATED WORKS

The long-standing problem of Oversquashing undermines the prowess of GNNs, which is evident in the tasks that require multi-hop interactions. The oversquashing is first observed by [7] in the ambit of message-passing of GNNs. Several research attempts were made to navigate the challenging terrain of oversquashing, like [8], [22]. Amidst all, rewiring emerged as the most enticing solution to tackle oversquashing. Earlier works like DropEdge [23] and GDC [24] perform rewiring operations to enable long-range information exchange. A different class of methods emerged with SDRF [10], GTR [14], BORF [25], and SJLR [26] characterize the exploration of edge-based curvatures. Those methods are non-differentiable and pursue sequential edge adjustments. The domain of spectral rewiring is further enriched with methods like FoSR [11] to introduce relational rewiring, distinguishing between added and existing edges while optimizing the spectral gap of the network. In a different vein, [27] combines the information-theoretic properties with spectral expansion to enable efficient rewiring. A newer direction unraveled with DiffWire [12] proposes an inductive differentiable rewiring strategy based on commute time, spectral gap, and effective resistance. The recently proposed LASER [13] sequentially rewires the graph, improving spatial connectivity and respecting the sparsity and locality of the input graph. Additionally, DRew [9] dynamically rewires the graph with a fixed delay in interactions among the neighbors. Another work, Co-GNN [28] performs layer-wise dynamic rewiring that learns when to update node features, highlighting asynchronous properties. A similar category of work [29] proposed aggregates information and updates after some fixed delay, which also satisfies the

asynchronous property. Another effective way to rewire is by converting the input into another graph by preserving the expander-type properties [30]. PR-MPNN [15] devised a rewiring strategy to construct a graph structure depending on the downstream tasks and underlying data distribution. The most recent work, PANDA [17] enhances the channel capacity of the nodes with higher importance to process a larger volume of information effectively to prevent oversquashing.

### 3 PROPOSED METHODOLOGY

#### 3.1 Preliminaries & Notations

Assume an attributed graph  $\mathcal{G} = (\mathcal{V}, \mathcal{E}, X, A)$  where  $\mathcal{V}$  denotes the set of nodes,  $\mathcal{E} \subseteq \mathcal{V} \times \mathcal{V}$  denotes the edge set,  $X \in \mathbb{R}^{n \times d}$  is the feature matrix containing  $d$ -dimensional node features, and  $A \in \mathbb{R}^{n \times n}$  is the adjacency matrix.

**Oversquashing** The effect of oversquashing is measured by the sensitivity bounds proposed by [8], [31]. The sensitivity bound is estimated as the Jacobian of  $h_v^{(l)}$  and  $h_u^{(0)}$  which is represented as,

$$\left\| \frac{\partial h_v^{(l)}}{\partial h_u^{(0)}} \right\|_1 \leq \underbrace{(cwp)^l}_{\text{model}} \underbrace{(\tilde{S}^l)_{uv}}_{\text{topology}}. \quad (1)$$

where  $c$  is the Lipschitz constant of the model parameters,  $w$  is the maximum entry of weight matrices, and the width  $p$ . Also, oversquashing is affected by the  $\tilde{S}^{(l)}$  where  $\tilde{S}$  can be a normalized adjacency matrix. The lower value of the bound signals diminished the effect on the message propagation of a node by its neighbors.

#### 3.2 Asynchronous Message Passing Framework

In this section, we will illustrate the generalized asynchronous message passing framework. The framework initially chooses a batch of nodes, say  $B$ , with  $|B| \leq n$  that satisfies some pre-defined criteria function  $\mathcal{C}$ . Thereafter, the framework updates the features of all nodes in  $B$ , and features for the rest of the nodes are kept unaltered. Suppose the feature of a node  $v \in B$  is updated at  $l^{th}$  layer, then it also crosses the time-stamp  $l$ . We assign every node a tuple representing the layer number and the corresponding time stamp. The following equation represents the asynchronous message-passing operation,

$$x_v^{(l+1, l+1)} = \begin{cases} \Phi_l \left( x_v^{(l_v, l)}, \sum_{u \in N(v)} \Psi_l(x_v^{(l_v, l)}, x_u^{(l_u, l)}) \right), & v \in B \\ x_v^{(l_v, l+1)}, & \forall v \notin B. \end{cases} \quad (2)$$

where  $\Psi_l, \Phi_l$  are respectively MESSAGE and COMBINE functions for  $l^{th}$  layer,  $l_v$  denotes the layer at which  $x_v$  is last updated with  $0 \leq l_v \leq l$ . If a node does not participate in the message-passing operation, then its time-stamp will increase by one, but the last updated layer remains unchanged. Importantly, the framework considers a node set which not necessarily need to be part of any subgraph, strictly differing from the methods pursuing subgraph sampling like [32], [33]

**Centrality-aware Asynchronous Message Passing (CAMP)** We propose a novel strategy to select node batches, prioritizing the importance of the nodes within a given network. In this context, the centrality values of nodes are considered as the selection criteria for creating node batches. We adopt five different well-recognized centrality measures: Degree [34], Betweenness [35], Closeness [36], Load [37], and PageRank [38] to serve the purpose. Initially, we estimate the centrality scores of each node in the pre-processing stage. Concurrently, we also assign ordering (either ascending or descending) of the centrality values, which confirms the monotone effects of the importance of nodes. For instance, the centrality of nodes in descending order can be presented as follows,

$$C_n = \{c^{(1)}, c^{(2)}, \dots, c^{(n)} : c^{(i+1)} \geq c^{(i)}, \forall 1 \leq i \leq n-1\}, \quad (3)$$

where  $c^{(i)}$  denotes the centrality of the node  $i$ . To generate a set of mini-batches, we divide the centrality values into  $L$  smaller subsets, where  $L$  denotes the total number of layers in the base GNN. At layer  $l$ , the subset  $C_n^{(l)}$  acts as our candidate node batch. The features of nodes in  $C_n^{(l)}$  will be updated. The  $l^{th}$  subset can be presented as,

$$C_n^{(l)} = \{c_l^{(1)}, c_l^{(2)}, \dots, c_l^{(m)} : c_l^{(i+1)} \geq c_l^{(i)}, \forall 1 \leq i \leq m-1\} \quad (4)$$

where  $c_k^{(i)}$  is the centrality of  $i^{th}$  node which belong to the  $l^{th}$  subset and  $m = |C_n^{(l)}| = \lfloor \frac{C_n}{L} \rfloor$  with  $l \in [1, L]$ . Note that each subset will maintain an identical order to  $C_n$ . The layer-specific disjoint batching of nodes ensures the participation of each node in the message-passing operation exactly once. We also offer a provision for selecting a portion of nodes from each subset  $C_n^{(l)}$ . Assuming a sampling probability is  $p$ , then the size of the node batch will be  $mp = |C_n^{(l)}|p$  where  $0 < p \leq 1$ . We term the framework as  $p$ -CAMP. If we sample a full batch at every layer, then our framework is termed as 1-CAMP or simply CAMP.

**Update Rule of CAMP** The feature update rule of CAMP can be defined as follows,

$$x_v^{(l+1,l+1)} = \begin{cases} \Phi_l \left( x_v^{(l,l)}, \sum_{u \in N(v)} \Psi_l(x_v^{(l,l)}, x_u^{(l,l)}) \right), & v \in C_n^{(l)} \\ x_v^{(l,l+1)}, & \forall v \notin C_n^{(l)}, \end{cases} \quad (5)$$

**Oversquashing Mitigation** CAMP selects centrality-guided node batches and asynchronously updates their features. These updates account for the older versions of the neighbors' features, which are already stored in the fixed-sized channels. The updated features of the current node batches may remain unchanged for a while and are later utilized by other node batches in the subsequent layers. The asynchronous updates ensure utilization of feature channels in a regular interval of time. Furthermore, the high centrality nodes act as roadblocks to the essential information propagation. The time-dependent access to these fixed-sized channels overcomes the constraints of channel capacity, facilitating the flow of information through high centrality nodes. Therefore, CAMP prevents the simultaneous storing of exponentially growing information in fixed-sized channels, mitigating the effects of oversquashing. To validate the efficacy of CAMP, we provide the following proposition.

**Proposition 3.1.** *For any nodes  $u, v$  with  $l$  distance apart, CAMP maintains a higher feature sensitivity bound compared to standard synchronous message passing.*

*Proof.* Assume in the  $l$ -th layer, CAMP uses the normalized adjacency matrix as  $\tilde{S}^{(l)}$ . Thus, reformulating Lemma 1 from [10], we have the following sensitivity bound,

$$\left\| \frac{\partial h_v^{(l)}}{\partial h_u^{(0)}} \right\|_1 \leq (cwp)^l \left( \prod_{j=1}^l (\tilde{S}^{(j)})_{uv} \right). \quad (6)$$

As CAMP applies disjoint node batches in each layer, then we have  $\tilde{S}^{(l_1)} \neq \tilde{S}^{(l_2)}, \forall l_1 \neq l_2$ . The right side of inequality in Eq. 6 represents products of the consecutive distinct adjacency matrices. Precisely, the oversquashing occurs for the decay of the term  $\tilde{S}_{uv}$  impacted by the power-normalized adjacency matrix. On the contrary, in Eq. 6, the directly powered adjacency matrix is not involved, but the products of consecutive distinct adjacency matrices are estimated. Thus, the possibility of small quantities occurring is lowered, signifying the control of oversquashing.  $\square$

**Order matters** High centrality nodes are assumed to be the pivotal source of information in a network. The descending order of centrality values ( $C_n$ ) allows higher centrality nodes to propagate vital information earlier. Subsequently, the lower centrality nodes access those previously estimated informative messages and utilize them without facing channel capacity constraints. In contrast, the ascending ordering does not provide such advantages for efficient message propagation. Notably, we achieved optimal performance with the descending order of centrality values throughout the experiments.

### 3.3 Properties of CAMP

**[1] Layer-wise Rewiring** CAMP updates the features of a particular set of nodes while the rest of the nodes remain unaffected. The edges adjacent to the candidate node batch remain connected, and the remaining edges are dropped. Therefore, the structure of the graph alters in each layer according to the selected node batches, unlike the existing sequential rewiring methods [11], [13], etc. Thus, CAMP leverages layer-specific rewiring and enables asynchronous message aggregation.

**[2] Variable Hop Aggregation** CAMP simulates a variable hop aggregation strategy, unlike the standard MP-GNNs. For any layer  $l$ , the corresponding candidate node batch  $C_l^n$  updates features from the neighbors, which can be either already updated in some previous layers ( $< l$ ) or will be updated in the upcoming layers ( $> l$ ). The updated features of the current node batch are the aggregated form of variable hops and the updated features of their corresponding neighbors. This variable hop aggregation is the key characteristic of the asynchronous message-passing frameworks.

**[3] Order matters: Ascending or Descending** The effectiveness of CAMP can be influenced by the order of the centrality values of the nodes. The descending order of the centrality values enables the aggregation of rich information through the high centrality nodes in earlier layers. Those updated node features are further utilized by lower centrality nodes, and information propagation is efficiently leveraged. Conversely, for the ascending order of centrality values, the lower centrality nodes will not be able to collect structural information like the high centrality nodes mentioned in the previous scenario. However, the features aggregated by those nodes may not be sufficient to provide the necessary information to higher centrality nodes. In this context, we experimented to study the impact of ordering on the performance of CAMP, which is demonstrated in Figure 2. The empirical analysis reveals that the descending order of set  $C_n$  yields better performance over the same for the descending order. Furthermore, nodes with high centrality connect a larger volume of edges, causing oversmoothing in deeper layers. For a descending order of  $C_n$ , the faster interaction of high-centrality nodes compared to lower ones is supposed to diminish the effect of oversmoothing.

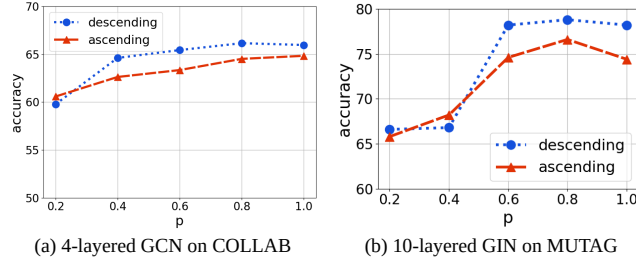


Fig. 2: The comparative study between the order of node centrality values on the performance of CAMP is presented. The performance is executed on the various batch sampling rates.

### 3.4 Complexity Analysis

The time complexity of CAMP-GNN only depends on the complexity of the underlying GNN model because the CAMP framework only adds an extra task of computing centrality scores performed as a pre-processing step. The cost of computing centrality values depends on the choice of centrality, like the cost of degree centrality is  $\mathcal{O}(|\mathcal{E}|)$ , the same for closeness is  $\mathcal{O}(|\mathcal{V}||\mathcal{E}|)$ , etc. Unlike PANDA, we do not increase the number of feature dimensions during message propagation; thus, the parameter complexity for CAMP-GNN also remains unaffected. Note that estimating node centrality can be computationally expensive for large-scale graphs. Thus, we bound our experiments within the molecular graphs which is also our key limitation.

### 3.5 Instances of CAMP

We will now illustrate the examples of CAMP-GNN by using GCN [18] and GIN [39]. The layer-wise update rule of CAMP-GCN is,

$$h_u^{(l+1,l+1)} = h_u^{(l,l)} + \sigma \left( \sum_{v \in N(v) \cap C_n^{(l+1)}} W^{(l+1)} h_v^{(l,l)} \right), \quad (7)$$

where  $W^{(l+1)}$  is the parameterized weight matrix. Observe that neighborhood aggregation is performed on the nodes that are neighbors and belong to the candidate node batch. Similarly, we define the update rule of CAMP-GIN as follows,

$$h_u^{(l+1,l+1)} = \text{MLP}_l \left( (1 + \epsilon) h_u^{(l,l)} + \sum_{v \in N(v) \cap C_n^{(l+1)}} W^{(l+1)} h_v^{(l,l)} \right), \quad (8)$$

where  $\text{MLP}_l$  denotes the combination of the linear layers with ReLU activation and  $\epsilon$  is the learnable parameter. In this case, the node features are also considered for aggregation if they belong to both the neighborhood and candidate batch.

TABLE 1: The performances of GCN and GIN coupled with CAMP are presented. The best and second-best results are respectively marked in green and blue colors.

Method	ENZYMES	MUTAG	PROTEINS	COLLAB	IMDB-BINARY	REDDIT-BINARY
GCN (None)	27.66 ± 1.16	72.15 ± 2.44	70.98 ± 0.73	33.78 ± 0.48	49.77 ± 0.81	68.25 ± 1.09
+ DIGL	27.51 ± 1.05	71.35 ± 2.39	70.60 ± 0.73	53.35 ± 0.29	49.91 ± 0.84	49.98 ± 0.68
+ SDRF	28.36 ± 1.17	71.05 ± 1.87	70.92 ± 0.79	33.44 ± 0.47	49.40 ± 0.90	68.62 ± 0.85
+ FoSR	25.06 ± 0.99	80.00 ± 1.57	73.42 ± 0.81	33.83 ± 0.58	49.66 ± 0.86	70.33 ± 0.72
+ BORF	24.70 ± 1.00	75.80 ± 1.90	71.00 ± 0.80	Time-out	50.10 ± 0.90	Time-out
+ GTR	27.52 ± 0.99	79.10 ± 1.86	72.59 ± 2.48	33.05 ± 0.40	49.92 ± 0.99	68.99 ± 0.61
+ CT-Layer	17.38 ± 1.03	75.89 ± 3.02	60.35 ± 1.06	52.14 ± 0.41	50.32 ± 0.94	51.58 ± 1.01
+ PANDA	<b>31.55 ± 1.23</b>	<b>85.75 ± 1.39</b>	<b>76.00 ± 0.77</b>	<b>68.40 ± 0.45</b>	<b>63.76 ± 1.01</b>	<b>80.69 ± 0.72</b>
+ CAMP (Ours)	<b>31.73 ± 2.30</b>	<b>80.80 ± 3.68</b>	<b>74.43 ± 1.64</b>	<b>69.86 ± 0.70</b>	<b>62.44 ± 2.15</b>	<b>84.96 ± 0.86</b>
GIN (None)	33.80 ± 0.11	77.70 ± 0.36	70.80 ± 0.82	72.99 ± 0.38	70.18 ± 0.99	86.78 ± 1.05
+ DIGL	35.71 ± 1.19	79.70 ± 2.15	70.75 ± 0.77	54.50 ± 0.41	64.39 ± 0.90	76.03 ± 0.77
+ SDRF	35.81 ± 1.00	78.40 ± 2.80	69.81 ± 0.79	72.95 ± 0.41	69.72 ± 1.15	86.44 ± 0.59
+ FoSR	29.20 ± 1.36	78.40 ± 2.80	73.10 ± 0.81	73.27 ± 0.41	71.21 ± 0.91	87.35 ± 0.59
+ BORF	35.50 ± 1.20	80.80 ± 2.50	73.70 ± 0.80	Time-out	71.30 ± 1.50	Time-out
+ GTR	30.57 ± 1.42	77.60 ± 2.84	73.13 ± 0.69	72.93 ± 0.42	71.28 ± 0.86	86.98 ± 0.66
+ CT-Layer	16.58 ± 0.90	56.85 ± 4.25	61.10 ± 1.18	52.30 ± 0.60	50.00 ± 0.97	54.58 ± 1.75
+ PANDA	<b>46.20 ± 1.41</b>	<b>88.75 ± 1.57</b>	<b>75.75 ± 0.85</b>	<b>75.11 ± 0.21</b>	<b>72.56 ± 0.91</b>	<b>91.05 ± 0.40</b>
+ CAMP (Ours)	<b>46.60 ± 2.26</b>	<b>83.40 ± 3.95</b>	<b>74.07 ± 1.73</b>	<b>74.14 ± 0.65</b>	<b>71.48 ± 1.47</b>	<b>89.24 ± 1.03</b>



TABLE 2: Results of GCN with None, SDRF, FoSR, BORF, and PANDA on PEPTIDES-FUNC and PEPTIDES-STRUCT. The best and second-best results are respectively marked in green and blue colors.

Method	PEPTIDES-FUNC(AP $\uparrow$ )	PEPTIDES-STRUCT(MAE $\downarrow$ )
GCN (None)	59.30 $\pm$ 0.23	0.3496 $\pm$ 0.0013
+ SDRF	59.47 $\pm$ 1.26	0.3478 $\pm$ 0.0013
+ FoSR	59.47 $\pm$ 0.35	0.3473 $\pm$ 0.0007
+ BORF	<b>59.94 <math>\pm</math> 0.37</b>	0.3514 $\pm$ 0.0009
+ PANDA	<b>60.28 <math>\pm</math> 0.31</b>	<b>0.3272 <math>\pm</math> 0.0001</b>
+ CAMP (Ours)	56.67 $\pm$ 0.76	<b>0.3138 <math>\pm</math> 0.0041</b>

## 4 EXPERIMENTS

### 4.1 Datasets

For graph classification, we considered six benchmark datasets, ENZYMES, MUTAG, PROTEINS, COLLAB, IMDB-BINARY, and REDDIT-BINARY, obtained from TUDatasets [40]. The details of the datasets are discussed in Section A of the Appendix.

### 4.2 Experimental Setup

We considered 6 datasets from TUDatasets [40] and 2 datasets from LRGB [5] to perform graph classification. We applied CAMP on the graphs with GCN and GIN as the base models. Performance is compared with several baselines: DIGL, SDRF, FoSR, BORF, GTR, CT-layer, and PANDA. We split each dataset into 80/10%/10% for the train. validation and test, respectively. For LRGB, the split will be 70%/15%/15%. We executed experiments on TUDatasets for 25 randomly generated splits and produced mean and standard deviations over the test sets, while the results of the LRGB datasets are averaged over four different random seeds. Our codebase is available at <https://github.com/kushalbose92/camp>.

### 4.3 Results & Discussions

The performance of CAMP paired with GCN and GIN is presented in Table 1, suggesting our proposed framework either outperforms all contenders or attains a second position, outperforming at least all rewiring methods. The consistent performance of CAMP establishes that oversquashing can be tackled by leveraging asynchronous message passing without distorting the original graph structure.

CAMP showed commendable improvements on REDDIT-BINARY, containing bigger graphs, where multiple bottleneck nodes are present. CAMP successfully enables the information propagation, eventually mitigating oversquashing. CAMP also outperformed on COLLAB, which contains a scientific collaboration network with a community structure. Our framework efficiently identifies key bottleneck nodes and enables message flow asynchronously to overcome channel constraints. CAMP is ranked as runner-up on MUTAG, PROTEINS, and IMDB-BINARY due to its smaller sizes, high sparsity, and lower number of bottleneck nodes. The asynchronous updates convert most of the nodes into an isolated state that plagues effective message passing. Furthermore, CAMP outperforms Peptide-struct as its features delineate structural information that differs from the features of Peptides-func, representing functional properties.

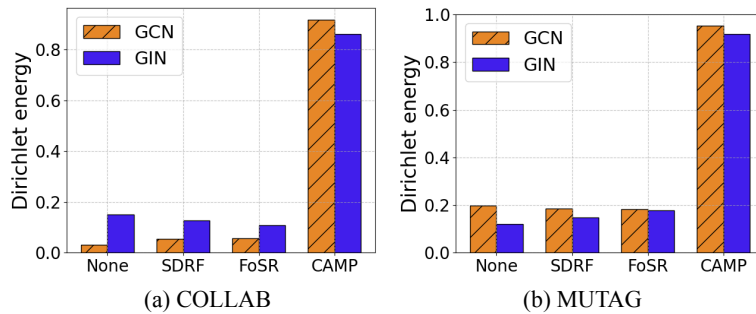


Fig. 3: A comparative study on the Dirichlet energies is presented. CAMP performs better than other rewiring methods.

### 4.4 Effect of Centrality Measure

We studied the effect of various node centrality measures on the performance of CAMP by applying 10-layered GCN and GIN to six datasets, with results demonstrated in Table 3. For instance, CAMP-GCN performed best on REDDIT-BINARY when closeness centrality was employed because the dataset contains larger graphs with a higher number of bottleneck nodes. Closeness centrality successfully identifies such nodes and attains optimal performance. In ENZYMES, nodes are amino acids, and closeness centrality identifies crucial amino acids that are effective for protein stability and functioning.

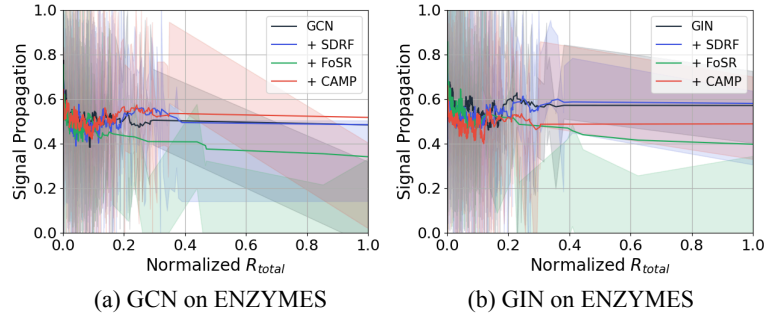


Fig. 4: The signal propagation with respect to normalized  $R_{\text{total}}$  is presented. CAMP maintains steady trends compared to others, with increasing resistance.

#### 4.5 Variation of Dirichlet Energy

We applied 10-layered GCN and GIN paired with CAMP on COLLAB and MUTAG and estimated the Dirichlet energies for the final layers. Figure 3 suggests Dirichlet energy for CAMP is higher than familiar rewiring methods like FoSR and SDRF. The node features remained distinguishable in deeper layers confirmed by the higher values of energies. The results clearly state that CAMP improves the model performance in the multi-layered GNNs without pursuing rewiring. Thus, we can claim that CAMP is capable of mitigating oversquashing and oversmoothing in multi-layered GNNs. More results are available in Section A of the Appendix.

#### 4.6 Signal Propagation

The total effective resistances ( $R_{\text{total}}$ ) [41] of the graph create hindrances to propagating information. A graph with higher effective resistance will likely grapple with oversquashing [14]. The efficacy of CAMP is measured with the signal propagation against the normalized  $R_{\text{total}}$  as adopted from [8]. Refer to Figure 4, which illustrates that CAMP performs better compared to other rewiring methods by effectively propagating the signal across the network with increasing effective resistance.

**Effect on Oversmoothing** We studied the effect of oversmoothing of multi-layered GCN and GIN on ENZYMES with various sampling rates of node batches. Figure 5 delineates the performance trends in the various network depths with varying  $p$ . CAMP demonstrated resilience to oversmoothing for the higher values of  $p$ . The performance strictly degrades when the CAMP is not applied, asserting the prowess of the proposed framework in mitigating oversmoothing in deeper GNNs. The higher number of layers increases the number of node batches, enhancing the number of time-stamps to access fixed channel capacity for processing aggregated features. Thus, CAMP mostly showed optimal performance when the network depth was higher. The results for the remaining datasets are provided in Section A of the Appendix.

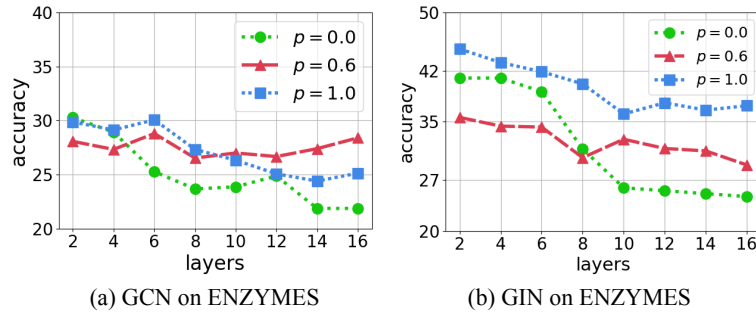


Fig. 5: The performance of CAMP in deeper layers is presented. The performance improved when the node batch sampling rate was increased.

#### 4.7 Variation of Batch Size

We attempted to study the impact of various node batch sampling rates  $p$  on the performance of GCN and GIN. The experiment is conducted on IMDB-BINARY, and classification accuracy is presented in Figure 6 for two different model depths. The trends illustrate that an increase in the sampling rate leads to an uptrend in performance. This is due to the larger number of nodes participating in the message-passing operation and aggregating more relevant information with the increasing  $p$ .

TABLE 3: The comparative performance of CAMP-GCN with five centrality measures. Best results are marked in Green.

Centrality	ENZYMES	MUTAG	PROTEINS	COLLAB	IMDB-BINARY	REDDIT-BINARY
Degree	28.93 $\pm$ 2.65	78.40 $\pm$ 4.46	72.00 $\pm$ 1.75	69.25 $\pm$ 0.71	58.52 $\pm$ 2.34	80.10 $\pm$ 0.90
Betweenness	30.20 $\pm$ 2.56	78.20 $\pm$ 4.20	71.54 $\pm$ 1.58	69.81 $\pm$ 0.82	58.24 $\pm$ 2.32	79.90 $\pm$ 0.94
PageRank	29.40 $\pm$ 2.37	<b>78.40 <math>\pm</math> 4.07</b>	71.14 $\pm$ 1.90	69.75 $\pm$ 0.86	<b>60.48 <math>\pm</math> 1.89</b>	81.28 $\pm$ 1.14
Load	31.13 $\pm$ 2.22	78.20 $\pm$ 4.16	72.11 $\pm$ 1.98	<b>69.86 <math>\pm</math> 0.70</b>	59.32 $\pm$ 1.95	79.94 $\pm$ 1.06
Closeness	<b>31.73 <math>\pm</math> 2.30</b>	77.60 $\pm$ 3.88	<b>74.43 <math>\pm</math> 1.64</b>	69.25 $\pm$ 0.83	59.52 $\pm$ 2.14	<b>84.96 <math>\pm</math> 0.86</b>

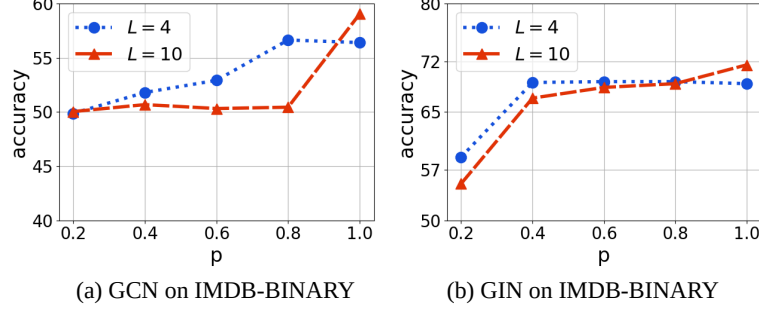


Fig. 6: The performance for various node batch sampling rates for two different numbers of model layers is presented. The performance improves when the sampling rate is higher.

## 5 CONCLUSION & FUTURE WORKS

We designed the generalized asynchronous message passing framework RAMP, which randomly selects node batches at every layer to update corresponding features. However, we identified the limitations of RAMP and proposed CAMP, which creates layer-specific node batches based on node centrality. Our proposed framework can be flexibly paired with a multitude of MP-GNNs. Furthermore, we also offer theoretical guarantees that CAMP is superior to RAMP in mitigating oversquashing. We applied CAMP to six standard graph datasets to validate the effectiveness of the framework. The experimental results indicate that CAMP demonstrated impressive performance, underscoring the prowess of asynchronous message passing over the structural rewiring. Exploring and designing asynchronous message-passing algorithms for dynamic graphs to alleviate oversquashing and oversmoothing can be potential future research directions.

## REFERENCES

- [1] F. Scarselli, M. Gori, A. C. Tsoi, M. Hagenbuchner, and G. Monfardini, "The graph neural network model," *IEEE transactions on neural networks*, vol. 20, no. 1, pp. 61–80, 2008.
- [2] F. Wu, A. Souza, T. Zhang, C. Fifty, T. Yu, and K. Weinberger, "Simplifying graph convolutional networks," in *International conference on machine learning*. PMLR, 2019, pp. 6861–6871.
- [3] G. Corso, L. Cavalleri, D. Beaini, P. Liò, and P. Veličković, "Principal neighbourhood aggregation for graph nets," *Advances in Neural Information Processing Systems*, vol. 33, pp. 13 260–13 271, 2020.
- [4] V. P. Dwivedi, C. K. Joshi, T. Laurent, Y. Bengio, and X. Bresson, "Benchmarking graph neural networks," 2020.
- [5] V. P. Dwivedi, L. Rampásek, M. Galkin, A. Parviz, G. Wolf, A. T. Luu, and D. Beaini, "Long range graph benchmark," in *Thirty-sixth Conference on Neural Information Processing Systems Datasets and Benchmarks Track*, 2022. [Online]. Available: <https://openreview.net/forum?id=in7XC5RqJEn>
- [6] S. Abu-El-Haija, B. Perozzi, A. Kapoor, N. Alipourfard, K. Lerman, H. Harutyunyan, G. Ver Steeg, and A. Galstyan, "Mixhop: Higher-order graph convolutional architectures via sparsified neighborhood mixing," in *international conference on machine learning*. PMLR, 2019, pp. 21–29.
- [7] U. Alon and E. Yahav, "On the bottleneck of graph neural networks and its practical implications," *arXiv preprint arXiv:2006.05205*, 2020.
- [8] F. Di Giovanni, L. Giusti, F. Barbero, G. Luise, P. Lio, and M. M. Bronstein, "On over-squashing in message passing neural networks: The impact of width, depth, and topology," in *International Conference on Machine Learning*. PMLR, 2023, pp. 7865–7885.
- [9] B. Gutteridge, X. Dong, M. M. Bronstein, and F. Di Giovanni, "Drew: Dynamically rewired message passing with delay," in *International Conference on Machine Learning*. PMLR, 2023, pp. 12 252–12 267.
- [10] J. Topping, F. Di Giovanni, B. P. Chamberlain, X. Dong, and M. M. Bronstein, "Understanding over-squashing and bottlenecks on graphs via curvature," *arXiv preprint arXiv:2111.14522*, 2021.
- [11] K. Karhadkar, P. K. Banerjee, and G. Montúfar, "Fosr: First-order spectral rewiring for addressing oversquashing in gnns," *arXiv preprint arXiv:2210.11790*, 2022.
- [12] A. Arnaiz-Rodríguez, A. Begga, F. Escolano, and N. Oliver, "Diffwire: Inductive graph rewiring via the lovász bound, 2022," URL <https://arxiv.org/abs/2206.07369>, vol. 2.
- [13] F. Barbero, A. Vellingker, A. Saberi, M. Bronstein, and F. Di Giovanni, "Locality-aware graph-rewiring in gnns," *arXiv preprint arXiv:2310.01668*, 2023.
- [14] M. Black, Z. Wan, A. Nayyeri, and Y. Wang, "Understanding oversquashing in gnns through the lens of effective resistance," in *International Conference on Machine Learning*. PMLR, 2023, pp. 2528–2547.
- [15] C. Qian, A. Manolache, K. Ahmed, Z. Zeng, G. V. d. Broeck, M. Niepert, and C. Morris, "Probabilistically rewired message-passing neural networks," *arXiv preprint arXiv:2310.02156*, 2023.
- [16] V. P. Dwivedi and X. Bresson, "A generalization of transformer networks to graphs," *arXiv preprint arXiv:2012.09699*, 2020.



- [17] J. Choi, S. Park, H. Wi, S.-B. Cho, and N. Park, "PANDA: Expanded width-aware message passing beyond rewiring," in *Forty-first International Conference on Machine Learning*, 2024.
- [18] T. N. Kipf and M. Welling, "Semi-supervised classification with graph convolutional networks," *arXiv preprint arXiv:1609.02907*, 2016.
- [19] P. Veličković, G. Cucurull, A. Casanova, A. Romero, P. Lio, and Y. Bengio, "Graph attention networks," *arXiv preprint arXiv:1710.10903*, 2017.
- [20] M. Chen, Z. Wei, Z. Huang, B. Ding, and Y. Li, "Simple and deep graph convolutional networks," in *International Conference on Machine Learning*. PMLR, 2020, pp. 1725–1735.
- [21] L. Faber and R. Wattenhofer, "GwAC: GNNs with asynchronous communication," in *The Second Learning on Graphs Conference*, 2023. [Online]. Available: <https://openreview.net/forum?id=zffXH0sEJP>
- [22] F. Di Giovanni, T. K. Rusch, M. M. Bronstein, A. Deac, M. Lackenby, S. Mishra, and P. Veličković, "How does over-squashing affect the power of gnns?" *arXiv preprint arXiv:2306.03589*, 2023.
- [23] Y. Rong, W. Huang, T. Xu, and J. Huang, "Dropege: Towards deep graph convolutional networks on node classification," *arXiv preprint arXiv:1907.10903*, 2019.
- [24] J. Klicpera, S. Weißenberger, and S. Günnemann, "Diffusion improves graph learning," *Advances in Neural Information Processing Systems*, vol. 32, pp. 13 354–13 366, 2019.
- [25] K. Nguyen, N. M. Hieu, V. D. Nguyen, N. Ho, S. Osher, and T. M. Nguyen, "Revisiting over-smoothing and over-squashing using ollivier-ricci curvature," in *International Conference on Machine Learning*. PMLR, 2023, pp. 25 956–25 979.
- [26] J. H. Giraldo, K. Skianis, T. Bouwmans, and F. D. Malliaros, "On the trade-off between over-smoothing and over-squashing in deep graph neural networks," in *Proceedings of the 32nd ACM International Conference on Information and Knowledge Management*, 2023, pp. 566–576.
- [27] P. K. Banerjee, K. Karhadkar, Y. G. Wang, U. Alon, and G. Montúfar, "Oversquashing in gnns through the lens of information contraction and graph expansion," in *2022 58th Annual Allerton Conference on Communication, Control, and Computing (Allerton)*. IEEE, 2022, pp. 1–8.
- [28] B. Finkelshtein, X. Huang, M. Bronstein, and u. u. Ceylan, "Cooperative graph neural networks," in *Proceedings of the 41st International Conference on Machine Learning*, ser. ICML'24. JMLR.org, 2024.
- [29] J. Chen, T. Liao, C. Chen, and Z. Zheng, "Improving message-passing gnns by asynchronous aggregation," in *Proceedings of the 33rd ACM International Conference on Information and Knowledge Management*, 2024, pp. 228–238.
- [30] A. Deac, M. Lackenby, and P. Veličković, "Expander graph propagation," in *Learning on Graphs Conference*. PMLR, 2022, pp. 38–1.
- [31] J. Topping, F. Di Giovanni, B. P. Chamberlain, X. Dong, and M. M. Bronstein, "Understanding over-squashing and bottlenecks on graphs via curvature," *arXiv preprint arXiv:2111.14522*, 2021.
- [32] W. L. Hamilton, R. Ying, and J. Leskovec, "Inductive representation learning on large graphs," in *Proceedings of the 31st International Conference on Neural Information Processing Systems*, 2017, pp. 1025–1035.
- [33] H. Zeng, H. Zhou, A. Srivastava, R. Kannan, and V. Prasanna, "Graphsaint: Graph sampling based inductive learning method," *arXiv preprint arXiv:1907.04931*, 2019.
- [34] S. P. Borgatti and D. S. Halgin, "Analyzing affiliation networks," *The Sage handbook of social network analysis*, vol. 1, pp. 417–433, 2011.
- [35] L. Freeman, "A set of measures of centrality based on betweenness.(1977)," *Sociometry*, vol. 40, no. 35–41, 1977.
- [36] L. C. Freeman *et al.*, "Centrality in social networks: Conceptual clarification," *Social network: critical concepts in sociology*. Londres: Routledge, vol. 1, pp. 238–263, 2002.
- [37] K.-I. Goh, B. Kahng, and D. Kim, "Universal behavior of load distribution in scale-free networks," *Physical review letters*, vol. 87, no. 27, p. 278701, 2001.
- [38] L. Page, S. Brin, R. Motwani, and T. Winograd, "The pagerank citation ranking: Bringing order to the web." Stanford InfoLab, Tech. Rep., 1999.
- [39] K. Xu, W. Hu, J. Leskovec, and S. Jegelka, "How powerful are graph neural networks?" *arXiv preprint arXiv:1810.00826*, 2018.
- [40] C. Morris, N. M. Kriege, F. Bause, K. Kersting, P. Mutzel, and M. Neumann, "Tudataset: A collection of benchmark datasets for learning with graphs," *arXiv preprint arXiv:2007.08663*, 2020.
- [41] A. Ghosh, S. Boyd, and A. Saberi, "Minimizing effective resistance of a graph," *SIAM review*, vol. 50, no. 1, pp. 37–66, 2008.
- [42] F. R. Chung, *Spectral graph theory*. American Mathematical Soc., 1997, vol. 92.

## APPENDIX

### DETAILS OF THE DATASETS

We considered six datasets collected from [40], and the details of the datasets are provided in Table 4.

TABLE 4: Details of six datasets are provided, which are obtained from TUDatasets.

Dataset	#train	#valid	#test	#avg nodes	#avg edges	metric	node feats
ENZYMES	480	60	60	32.63	124.27	accuracy	yes
MUTAG	150	18	20	17.93	39.58	accuracy	yes
PROTEINS	890	111	112	39.05	145.63	accuracy	yes
COLLAB	4000	500	500	74.49	4914.43	accuracy	no
IMDB-BINARY	800	100	100	19.77	193.66	accuracy	no
REDDIT-BINARY	1600	200	200	429.62	995.51	accuracy	no

### EXPERIMENTAL SETUP

We executed experiments on the base GNN models coupled with CAMP on the 25 random splits. For each split, the trained model is applied to the test set. The final test accuracy is presented with mean and standard deviation over all splits. The standard deviations are further scaled by the formula  $s.d. \times \frac{2}{\sqrt{T}}$  where  $T$  is the total number of random trails (here  $T = 25$ ), which is also followed by [11]. Among the datasets, COLLAB, IMDB-BINARY, and REDDIT-BINARY do not have node features. As per the standard policy, we assigned ones as the features to every node.

TABLE 5: The hyperparameters for each dataset are provided to reproduce the best results.  $L$  denotes the number of message-passing layers of the underlying GNN.

Model	ENZYMES		MUTAG		PROTEINS		COLLAB		IMDB-BINARY		REDDIT-BINARY	
	L	Centrality	L	Centrality	L	Centrality	L	Centrality	L	Centrality	L	Centrality
GCN	10	Closeness	16	Degree	16	Degree	10	Load	12	Pagerank	16	Closeness
GIN	10	Closeness	12	Degree	16	Closeness	12	Betweenness	10	Pagerank	12	Closeness

## HYPERPARAMETER DETAILS

The models are trained with a learning rate of 0.001 and a dropout rate of 0.50. Model parameters are optimized with Adam, and weight decay is fixed at  $10^{-5}$ . In each experiment, we employed both 4-layered GCN and GIN models with a batch size of 64. These are the fixed hyperparameters for the entire experiment. The other data-specific hyperparameters are provided in Table 5.

## DIRICHLET ENERGY

Let us consider graph  $G$  with adjacency matrix  $A$  and symmetrically normalized graph Laplacian  $\tilde{L} = I - \tilde{D}^{-\frac{1}{2}} \tilde{A} \tilde{D}^{-\frac{1}{2}}$ , then the Dirichlet energy [42] of the set of features  $X$  with Laplacian is represented as following,

$$\begin{aligned} \text{DE}(X, \tilde{L}) &= \text{Tr}(X^\top \tilde{L} X) \\ &= \frac{1}{2} \sum_{(i,j) \in \mathcal{E}} A_{ij} \left( \frac{X_i}{\sqrt{d_i}} - \frac{X_j}{\sqrt{d_j}} \right)^2 \end{aligned} \quad (9)$$

The Dirichlet energy is directly connected with the measure of oversmoothing in the GNNs. The lower value of DE indicates that the node features became indistinguishable when neighborhood aggregation was performed in the deeper layers. In our experiments, we utilized the Eq. 9 to compute the energies at the final layer of the architectures.

## SIGNAL PROPAGATION AND TOTAL EFFECTIVE RESISTANCE

We will present the estimation of signal propagation across the graph with respect to the normalized total effective resistance as discussed in the Experiments. For any input graph, first, consider a source node  $v$  and assign a  $p$ -dimensional feature vector with zero vectors assigned to the rest of the nodes. Initialize a model randomly with  $m$  layers, then the amount of signal propagated can be estimated as,

$$h_{\odot}^{(m)} = \frac{1}{p \max_{u \neq v} d_G(u, v)} \sum_{j=1}^p \sum_{u \neq v} \frac{h^{(m),j}}{\|h^{(m),j}\|} d_G(u, v) \quad (10)$$

where  $h^{(m),j}$  denotes the  $j^{th}$  component of the feature at the  $m^{th}$  layer,  $d_G(u, v)$  is the shorted distance between the node  $u$  and  $v$ . The normalized signal  $\frac{h^{(m),j}}{\|h^{(m),j}\|}$  weighted by  $d_G(u, v) / \max_{u \neq v} d_G(u, v)$  is propagated from source node  $v$  to all other nodes. The final signal is averaged over the number of feature dimensions  $p$ . In our context, for each graph, we selected 10 source nodes and the final signal  $h_{\odot}^{(m)}$  with total effective resistance averaged over each source node. This process is continued over all graphs, and total effective resistance and signal propagation are plotted.

## ADDITIONAL EXPERIMENTAL RESULTS

### Effect on Centrality on Performance of CAMP-GIN

We presented the comparative study of the performance of CAMP-GIN in Table 6. The experiment is conducted on a 10-layered GIN architecture. The optimal performances for each dataset are attained for different centrality measures, highlighting the importance of centrality choices.

TABLE 6: A comparative study of the performance of CAMP-GIN is presented based on five different centrality measures.

Centrality	ENZYMES	MUTAG	PROTEINS	COLLAB	IMDB-BINARY	REDDIT-BINARY
Degree	43.13 $\pm$ 2.88	<b>80.00 <math>\pm</math> 4.36</b>	72.39 $\pm$ 1.89	72.34 $\pm$ 0.77	70.64 $\pm$ 1.68	75.38 $\pm$ 1.13
Betweenness	41.87 $\pm$ 2.62	77.00 $\pm$ 4.16	72.07 $\pm$ 2.02	<b>73.30 <math>\pm</math> 0.86</b>	69.76 $\pm$ 2.15	72.70 $\pm$ 0.90
PageRank	41.00 $\pm$ 2.54	74.00 $\pm$ 4.08	72.68 $\pm$ 1.55	72.66 $\pm$ 0.79	<b>71.48 <math>\pm</math> 1.47</b>	77.98 $\pm$ 1.37
Load	39.93 $\pm$ 2.44	76.00 $\pm$ 4.28	72.64 $\pm$ 2.26	72.97 $\pm$ 0.85	69.84 $\pm$ 1.94	72.82 $\pm$ 0.78
Closeness	<b>46.60 <math>\pm</math> 2.26</b>	76.20 $\pm$ 2.96	<b>74.07 <math>\pm</math> 1.73</b>	72.57 $\pm$ 0.61	71.00 $\pm$ 1.99	<b>81.98 <math>\pm</math> 1.20</b>

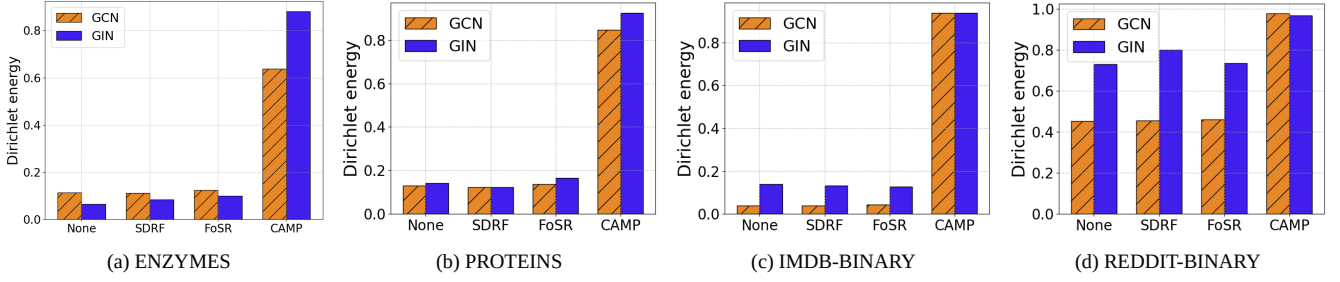


Fig. 7: The Dirichlet energies of the last layer of the models are presented. CAMP attains better energy values than other rewiring methods.

### Effect on Dirichlet Energy

The additional results are presented in Figure 7, where CAMP produces higher Dirichlet energy compared to other rewiring methods. Thus, CAMP showed the capacity to control oversmoothing in GNNs.

### Effect on Oversmoothing

The additional plots for the performance of CAMP in deeper layers are presented in Figure 8. The performance trends suggest the power of CAMP in tackling oversmoothing in the deep GNNs.

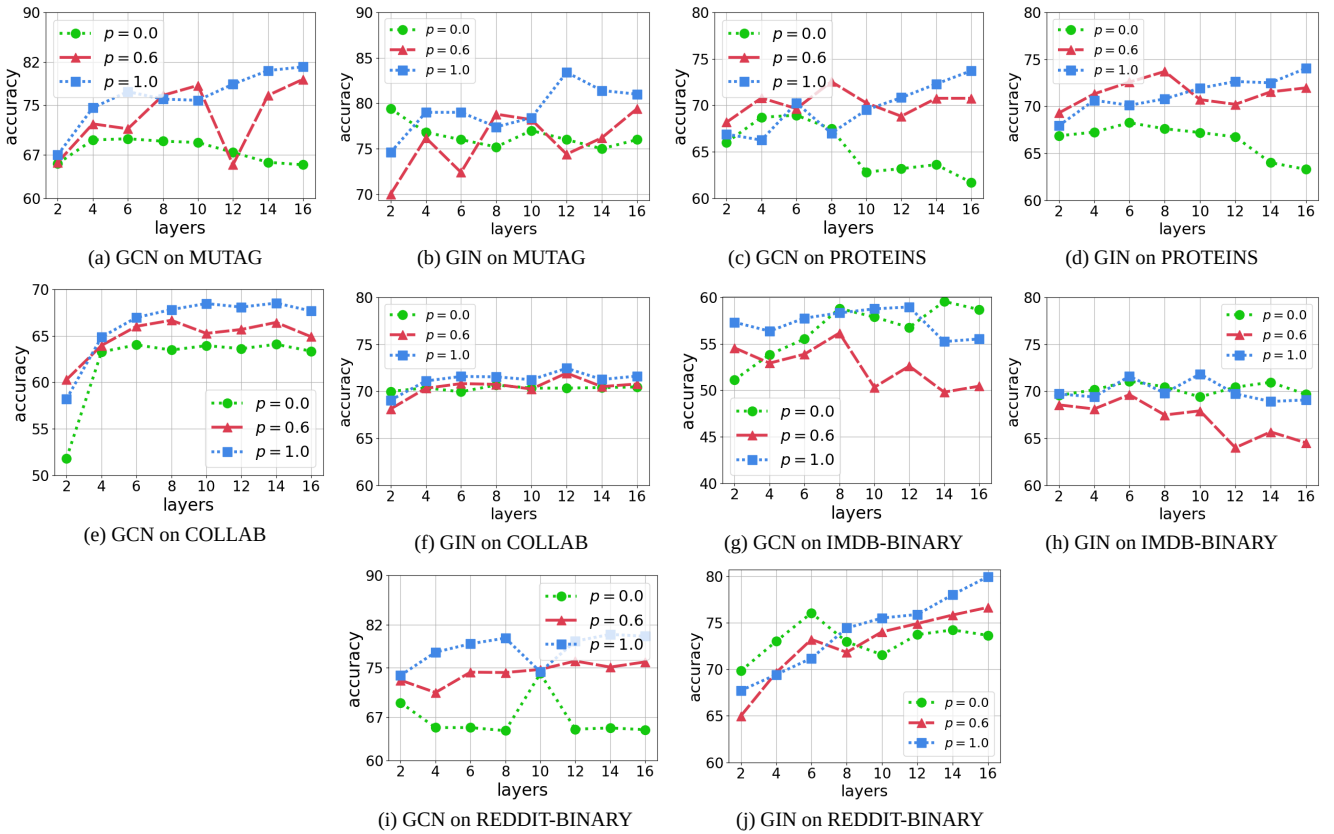


Fig. 8: Performance of CAMP with different batch sampling rates are presented for various network depths. The test accuracy is observed when the full subset is selected as the node batches.

### Signal Propagation

The additional results pertaining to the efficiency of CAMP in propagating signal are presented in Figure 9.

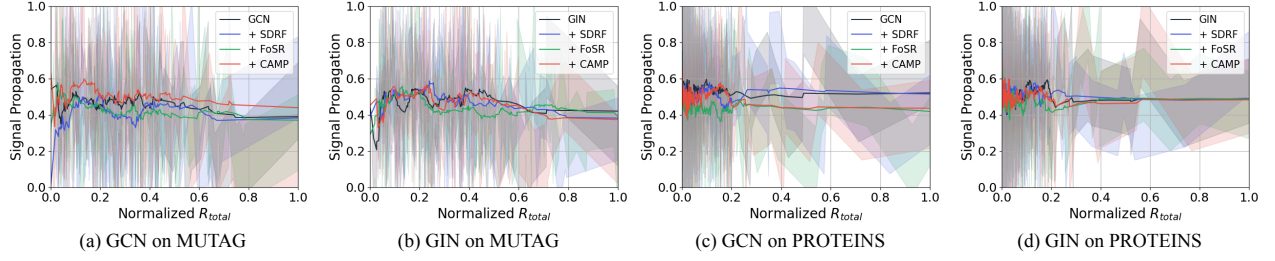


Fig. 9: The signal propagation with respect to normalized  $R_{out}$  is presented for MUTAG and PROTEINS. CAMP exhibited competitive performance compared to other rewiring methods by propagating a steady signal across the network with increasing resistance.

### Effect on Variation of Batch

The additional results of the performance of GCN and GIN paired with CAMP are presented over various sampling probabilities. The experiments are performed for two different layers 4 and 10. The plots are demonstrated in Figure 10. CAMP achieved best performance in most cases when the sampling probability is 1, indicating the full subset is chosen at a particular layer.

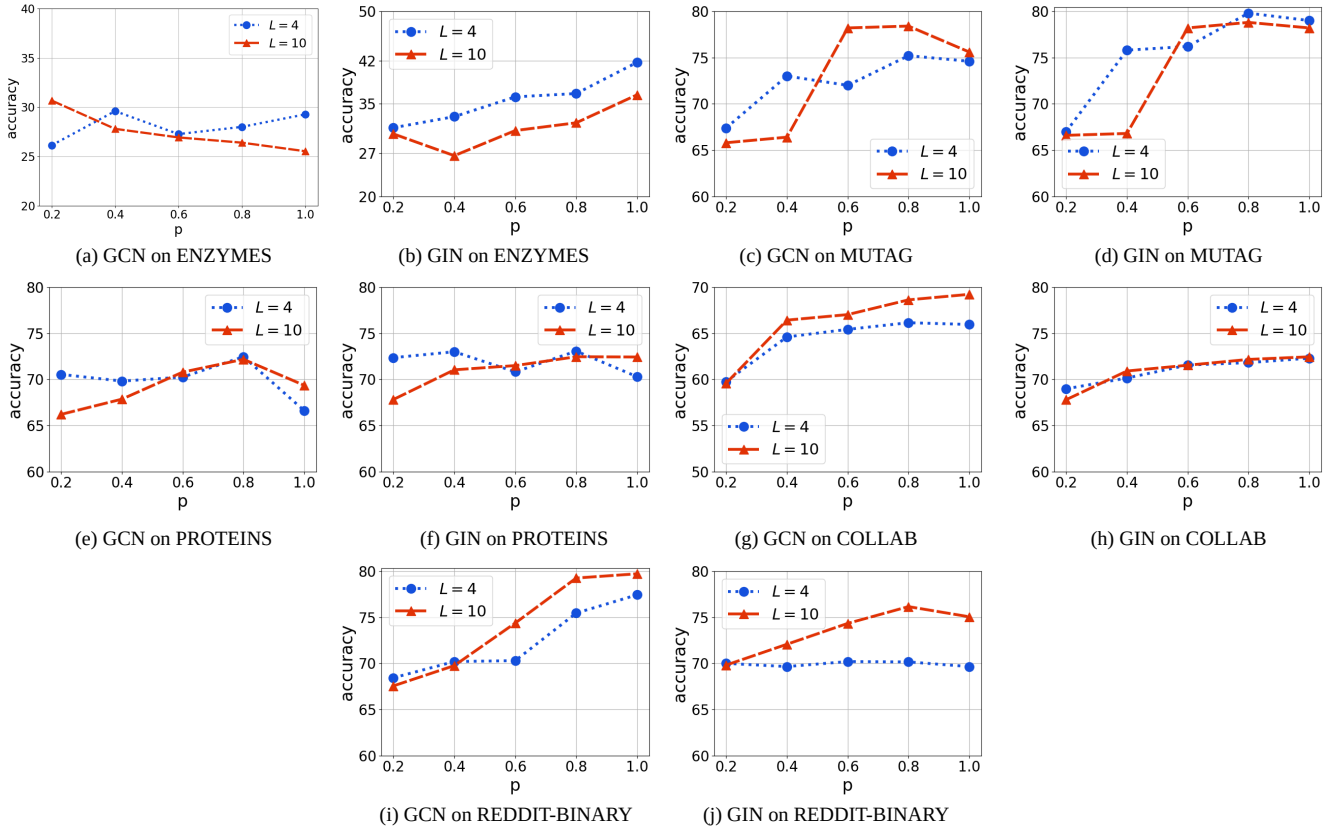


Fig. 10: The performance variation is illustrated with various node batch sampling rates. The best results are mostly obtained when the complete subset is chosen as a node batch for the hidden layers.